UNEC Journal of Engineering and Applied Sciences
Vol. 4, No.2, 2024, pp. 37-46
DOI: https://doi.org/10.61640/ujeas.2024.1204

SECTION: PHYSICAL SCIENCES

Formation of $CrSi_2$ film and measurement of optical band gap energy

K.T. Dovranov[1], G.T. Imanova[2,3,*], V.V. Loboda[4], M.T. Normuradov[1], I.R. Bekpulatov[1]

[1]*Karshi State University, 17 Kuchabag street, Karshi 180119, Uzbekistan*
[2]*Institute of Radiation Problems, Ministry of Science and Education Republic of Azerbaijan, 9 B.Vahabzade str., Baku AZ1143, Azerbaijan*
[3]*Khazar University, Department of Physics and Electronics, 41 Mahsati Str., Baku AZ1096, Azerbaijan*
[4]*Peter the Great St. Petersburg Polytechnic University, 29B Polytechnicheskaya, St. Petersburg 195251, Russia*
e-mail: gunel_imanova55@mail.ru

Abstract

The surface morphology and natural composition of the movies were analyzed for different temperature conditions. Thin films of $CrSi_2$/Si(111) were formed on polished substrates heated to 480 K using a special heater in a vacuum of $1.2 \cdot 10^{-4}$ mbar by the solid-phase ion-plasma method. During the experiment, the substrates were mounted on a rotating carousel holder at a distance of 150 mm from the surface of the magnetron target. The magnetron power supply current is 716 mA, power 263 W, voltage 320 V. Thin films of $CrSi_2$ are formed from a $CrSi_2$ target with a purity of 99.5% by the solid-phase ion-plasma method. The measurement results show that the elemental stoichiometric composition of thin $CrSi_2$ films grown by the solid-phase ion plasma method is Si/Cr = 33.6/62.32, which confirms the formation of chromium disilicide. Using optical spectroscopy methods, the widths of indirect and direct band gaps of amorphous and nanostructured thin films of chromium disilicide grown by the ion-plasma method in high vacuum were determined, and a comparative analysis was carried out with theoretically determined values based on the theories of Townes, Kumar, and Kubelka-Munk. The results showed that the band gap for Si(111) and $CrSi_2$ polycrystalline films is 1.1512 eV and 0.3543 eV. Tauc plots show that $CrSi_2$ thin films have an indirect band gap (energy of indirect allowed optical transitions): $E^{opt}_{g.ind}$=0,064 eV and $E^{opt}_{g.ind}$ =0,068 eV, respectively, and direct band gap (energy of direct allowed optical transitions) $E^{opt}_{g.ind}$ =0,354 eV and $E^{opt}_{g.ind}$ =0,368 eV. This research serves to enhance scientific research on band gap determination of silicide thin films.

Keywords: ion-plasma magnetron sputtering, chromium disilicide, band gap, Tauc plot, amorphous and nanostructured films.
PACS numbers: 52.35.Py, 52.55.Tn

Received:	*Revised:*	*Accepted:*	*Published:*
19 September 2024	*3 November 2024*	*7 November 2024*	*26 December 2024*

1. Introduction

The optical bandgap is a vital characteristic of semiconductor materials [1]. Something else, the zone is called “indirect” transmission capacity [2].

To degree the optical properties of semiconductors, a UV spectrometer is utilized, which comprises of a light source of the desired ghostly run and a gadget for measuring the transmittance of KBr unmistakable and IR spectra, with a monochromator.

Specular reflection is coordinate radiation from the surface of the film, comparing to Snellius law of reflection. Diffuse reflection (DR) is the wavelength-dependent retention of radiation occurrence and scattered on a film and inside a fabric. A few of this radiation in the long run clears out the bulk test in all bearings. Measuring diffuse reflectance employing a UV spectrophotometer could be a standard method for deciding the optical properties of lean movies [3-10].

In specific, E_g is an imperative property of semiconductor nanofilms that decides their appropriateness in optoelectronic applications. In DR spectroscopy, there are numerous strategies for getting lean movies [11-17].

The thought of utilizing DR spectra gotten from semiconductor nanostructures to calculate the band hole was to begin with proposed by the Kubelka-Munk hypothesis [12]. The hypothesis at first portrays the development of light inside a light diffusing design and is based on two differential conditions:

$$\left.\begin{aligned} -di &= -(S+K)idx + Sjdx \\ -dj &= -(S+K)jdx + Sidx \end{aligned}\right\} \tag{1}$$

The Kubelka-Munk hypothesis is substantial for molecule sizes comparable to or littler than the wavelength of occurrence light, and DR does not take under consideration the auxiliary commitments of reflection, refraction and diffraction. In case the thickness of the sample is inside worthy limits, it'll not influence the reflection. Therefore, the Kubelka-Munk equation can be written for any wavelength:

$$\frac{K}{S} = \frac{(1-R_\infty)^2}{2\cdot R_\infty} = F(R_\infty) \tag{2}$$

If the incident radiation is perfectly scattered, the absorption coefficient K is 2α. In this case, assuming that the scattering coefficient S is constant with respect to the wavelength, the Kubelka-Munk function is proportional to the absorption coefficient α, and applying equation (2), we obtain the following relation [18-20]:

$$[F(R_\infty)h\nu]^2 = A\left(h\nu - E_g\right) \tag{3}$$

In this work, the band gap (E_g) of chromium silicide films was determined based on the Tauc relation given in equation (3). For a direct gap semiconductor material, the Tauc relation is given by:

$$\alpha(h\nu)\cdot h\nu = A\cdot(h\nu - Eg)^n \tag{4}$$

Where α is the linear absorption coefficient, ν is the frequency of light, A is the proportionality constant. n is an indicator that determines the type of interband transitions, n is taken equal to 1/2 for materials with a direct bandgap (1/2; 3/2; 5/2; 2 and 3 for direct and indirect allowed and forbidden transitions, respectively). The spectral dependences of the absorption coefficient *α(hν)* were calculated using the following analytical equations using the formulas [21-25]:

$$\alpha(h\nu) = \frac{ln\left(\frac{R_{max}-R_{min}}{R_{(h\nu)}-R_{min}}\right)}{2\cdot d} \tag{5}$$

2. Experiments

Experimental samples of chromium silicide were obtained by the ion-plasma method using an improved EPOS-PVD-DESK-PRO magnetron sputtering installation [26-27], the diagram of which is shown in figure 1.

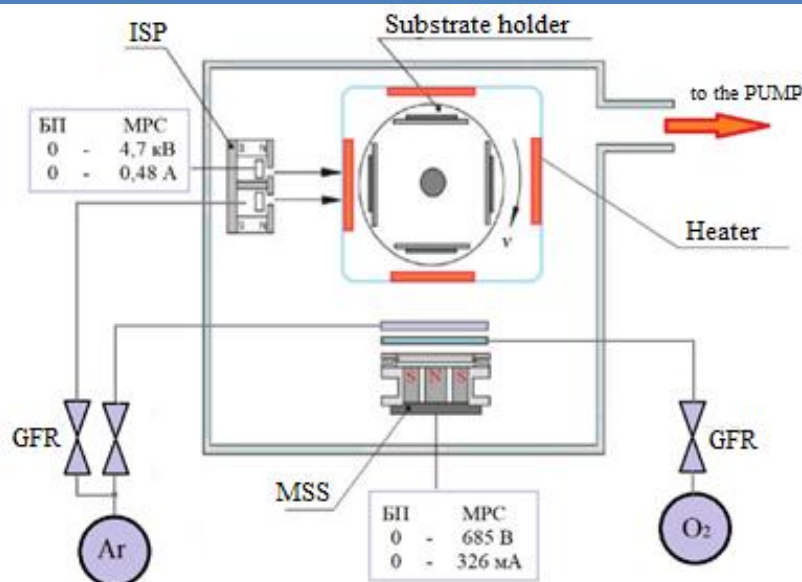

Figure 1. Diagram of the experimental setup for the formation of a $CrSi_2$ film by the solid-phase ion-plasma method: ISP - ion source for purification, MSS - magnetron sputtering system, GFR - gas flow regulator

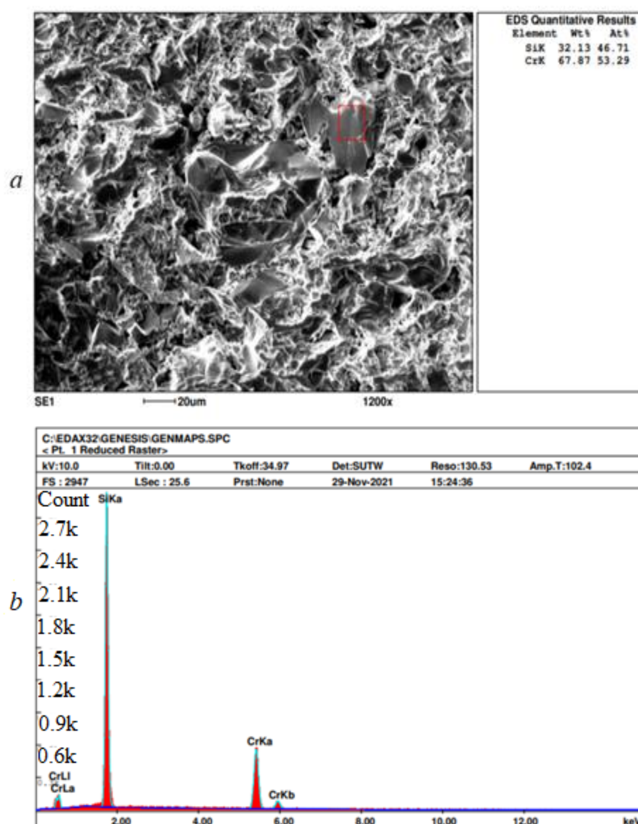

Figure 2. Results of studying the $CrSi_2$ target using a scanning electron microscope: SEM image of the surface (a) and EDX spectrum (b)

Before applying the film, the surface of the silicon wafers was subjected to a two-stage treatment: primary cleaning with 30% diluted hydrofluoric acid, then the surface was subjected to secondary cleaning with a high-energy Ar^+ ion-plasma flow inside the magnetron chamber. Thin films of $CrSi_2$/Si(111) were formed on polished substrates heated to 480 K using a special heater in a vacuum of $1.2 \cdot 10^{-4}$ mbar by the solid-phase ion-plasma method. During the

experiment, the substrates were mounted on a rotating carousel holder at a distance of 150 mm from the surface of the magnetron target. The magnetron power supply current is 716 mA, power 263 W, voltage 320 V. Thin films of $CrSi_2$ are formed from a $CrSi_2$ target with a purity of 99.5% by the solid-phase ion-plasma method (figure 2a). Elemental analysis of the $CrSi_2$ target was performed using energy dispersive spectroscopy (figure 2b).

3. Results and discussion

X-ray spectroscopy is an essential tool for analyzing the structure and materials' elemental and chemical composition [28-33]. The elemental composition of the films was studied using energy-dispersive X-ray spectroscopy (EDX). In figure 5 shows an SEM image of the surface of the $CrSi_2$ film. The studies were carried out using a Quanta 200 scanning electron microscope. Table 1 shows the percentage of elements in the $CrSi_2$ film.

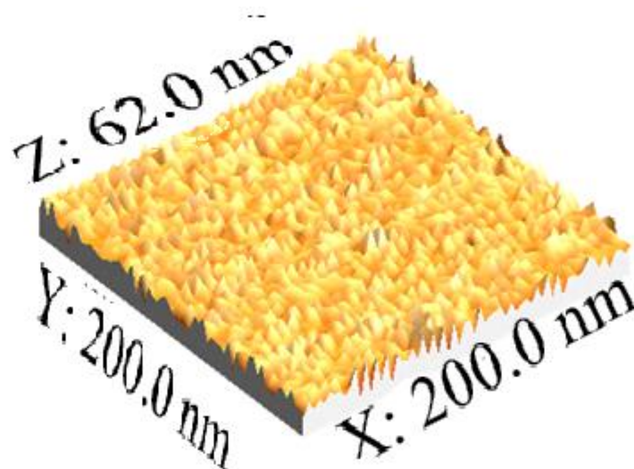

Figure 3. Three-dimensional images of the surface of $CrSi_2$ thin films obtained by atomic force microscopy

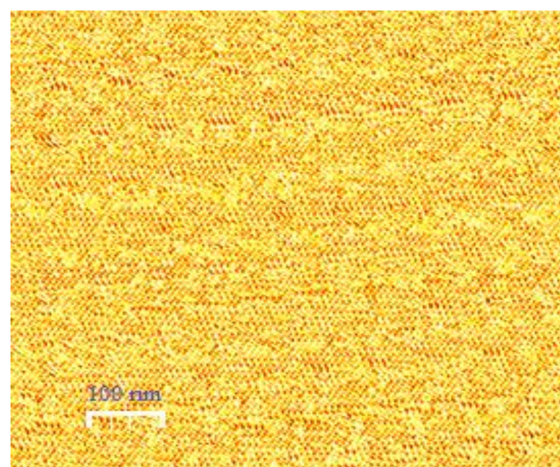

Figure 4. Two-dimensional images of the surface of $CrSi_2$ thin films obtained by atomic force microscopy

According to the results of measurements using energy dispersive X-ray spectroscopy (EDX), the elemental composition of the films is as follows: Si - 33.6%, Cr - 62.32% and a very small amount of O - 4.08%. As can be seen from the information displayed, the test contains the foremost chromium and silicon by mass and nuclear rate and exceptionally small oxygen.

The table appears that oxygen is display within the littlest amount. The arrangement of $CrSi_2$ lean movies on the silicon surface can be clarified based on the stoichiometry comes about.

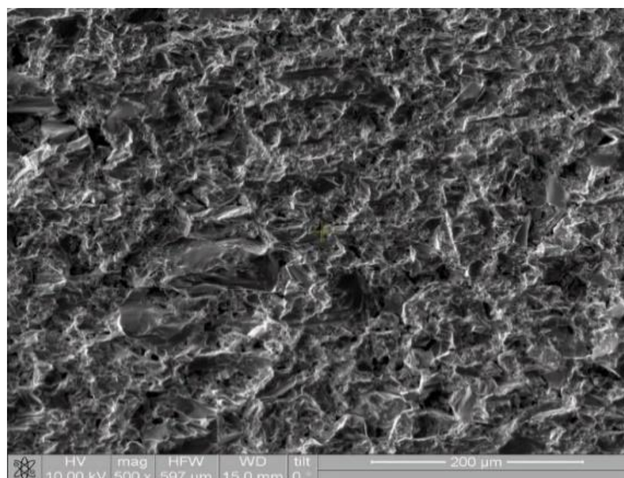

Figure 5. SEM image of the surface of the synthesized film

Quantitative results of energy dispersive analysis		
Element	Mass	at. %
SiK	36,35	33,6
CrK	60,4	62,32
OK	3,25	4,08

Table 1. Elemental composition of the sample

To study the distribution of elements, the film surface was examined at an angle of 48 degrees. To study the internal structure of the sample, a cross section of the $CrSi_2$/Si boundary was taken.

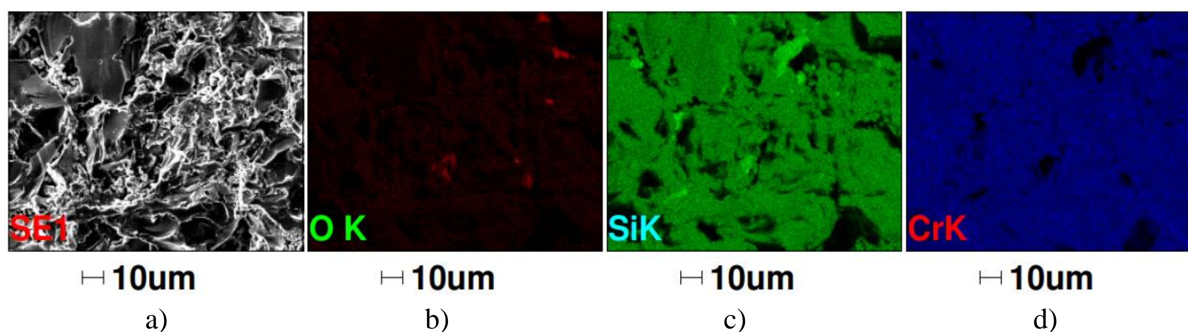

a) b) c) d)

Figure 6. Image elemental composition map:
a) Depth profile of a $CrSi_2$ film b) image of the low amount of oxygen in the sample c) image of the presence of Si in the film d) depth profile of Cr in a thin film

Much obliged to this, a picture of the conveyance of components along the profundity of the test was gotten (figure 6). As can be seen within the photo, the test contains on the surface: chromium, silicon and an awfully little sum of oxygen. SEM pictures of the film surfaces appear that the $CrSi_2$ film shaped by the solid-phase particle plasma strategy is nebulous. To get a polycrystalline film structure, extra warm treatment is fundamental. Heat treatment was carried out at 680 K for 1.3 hours.

Constrained by data around the vitality structure and the nature of interband moves within the $CrSi_2$ film, equation (4) was gotten by approximating the retention information gotten utilizing the Kumar and Kubelka-Munk models, accepting the parameter n to be a variable esteem. The best fit (correlation coefficient was 0.986) was achieved with n values of 2 and 0.5 for $CrSi_2$. Figure 7 shows the spectral dependences of absorption in the coordinates of optical transitions based on the Kubelka-Munk and Kumar approach, calculated using formulas (2) and (4). Based on these dependencies, the values of the band gap (optical band gap) were obtained. Approximation of the linear range of the spectral dependence by a straight line up to the intersection with the x-axis gives values of 1.1512 eV and 0.3543 eV for Si(111) and $CrSi_2$/Si(111) thin films, respectively.

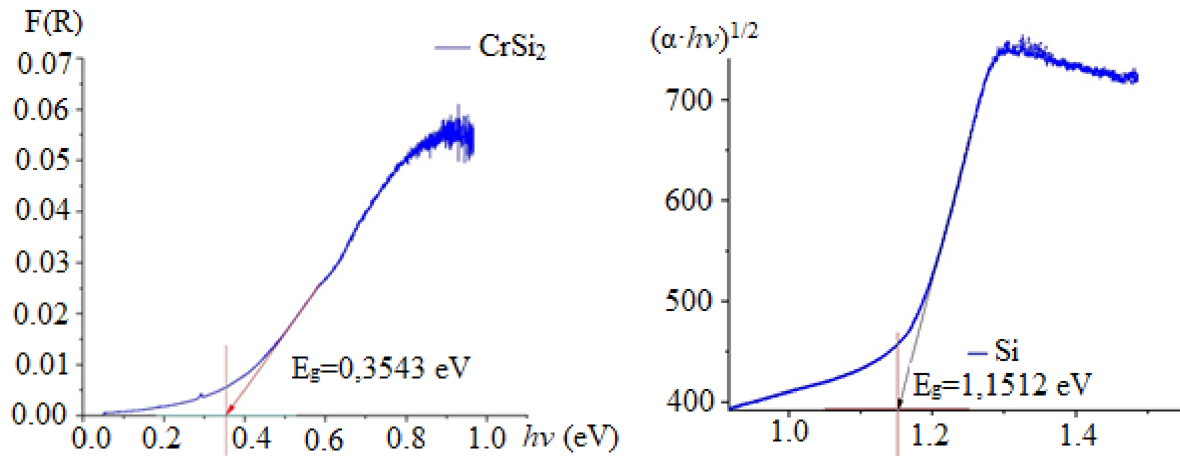

Figure 7. Tauc plot for $CrSi_2$ and Si thin films for indirect transition according to the Kubelka-Munk model

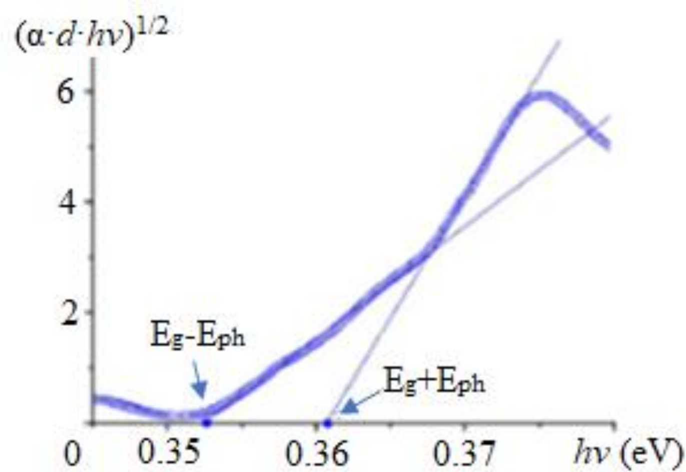

Figure 8. Energy gap values with absorption and phonon emission (E_{ph}) according to the Kumar model for chromium silicide

The reason of this work is to think about the morphology, basic composition and optical and electronic characteristics lean movies of $CrSi_2$ gotten by the solid-phase ion-plasma strategy (figure 8).

To degree the band hole of lean chromium disilicide movies gotten by the solid-phase ion-plasma strategy utilizing IR retention and UV spectroscopy, the dependences of the UV retention coefficient and refractive records of the movies on the vitality of occurrence photons were measured (figure 9).

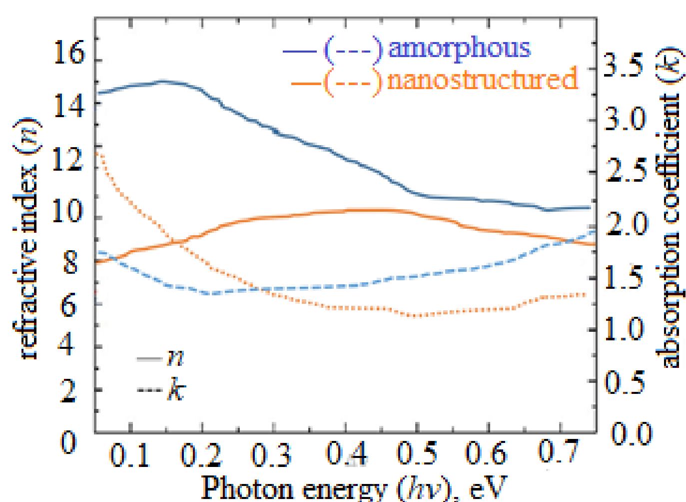

Figure 9. Refractive index and extinction coefficient of films as a function of photon energy: – (---) amorphous (sputtered) and – (---) nanostructured (heated)

The optical electronic band gaps of amorphous and polycrystalline $CrSi_2$ thin films were determined by measuring the IR reflectance and transmittance of 62 nm thick $CrSi_2$ deposited on an E_g^{opt} silicon substrate. The direct and indirect optical band gap values were determined using Tauc plots, figure 10. A sharp increase in photon energy above 0.063 and 0.34 eV can be observed for amorphous and nanostructured $CrSi_2$ thin films, respectively, which confirms the semiconductor properties of polycrystalline $CrSi_2$ films. Tauc plots show that $CrSi_2$ thin films have an indirect band gap (energy of indirect allowed optical transitions): $E_{g.ind}^{opt} = 0{,}064$ eV and $E_{g.ind}^{opt} = 0{,}068$ eV, respectively, and direct band gap (energy of direct allowed optical transitions) $E_{g.dir}^{opt} = 0{,}354$ eV and $E_{g.dir}^{opt} = 0{,}368$ eV. The instability was assessed based on a straight relapse fit to the chosen information extend. Hence, lean movies of shapeless $CrSi_2$ are narrow-gap semiconductors, which clarifies the moo electrical resistance and semimetal-like behavior. With fractional crystallization, an increment within the band hole can be observed, although its esteem isn't rise to to that of single-crystal $CrSi_2$ (0.35 eV). The coming about electronic structure is reliable with an increase in electrical resistance and a diminish within the measured carrier concentration, which can be clarified by a diminish within the level of abandons and nanostructuring amid tempering. Such changes within the electronic structure of $CrSi_2$ lean movies due to crystallization are steady with other optical transmittance estimations [34-39].

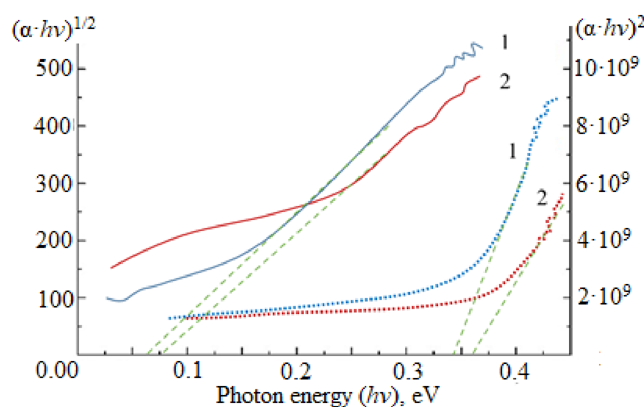

Figure 10. Tauc diagrams for indirect and direct band gaps of amorphous (sputtered) and nanostructured (annealed) $CrSi_2$ thin films.

1 — Amorphous film, 2 — Nanostructured film. The green dotted lines show the linear fit to the Tauc plot.

The hv esteem compares to the width of the tails of localized states close the band edge and is gotten from the variety plot close the band hole E_U. Due to the diminish within the imperfection level ln(α), a sharp diminish in nano crystallization is watched with E_U values of 0.163 eV and 0.346 eV for the sputtered and strengthened movies, separately. In this way, the band tails are nearly indistinguishable to the E_U band crevice values and can clarify the quasi-metallic behavior of undefined lean movies.

The gotten values of the vitality crevice and phonon vitality for lean movies of Si(111) and $CrSi_2$/Si(111) are summarized in table 2.

Sample / Method	Si (111)	$CrSi_2$
	E_g (eV)	E_g (eV)
Kubelka-Munk	1,1512	0,3543
Kumar	1,132	0,362
Tauca	-	0,346
Experiment	1,14	0,34

Table 2. Band gap values of thin films determined by different methods

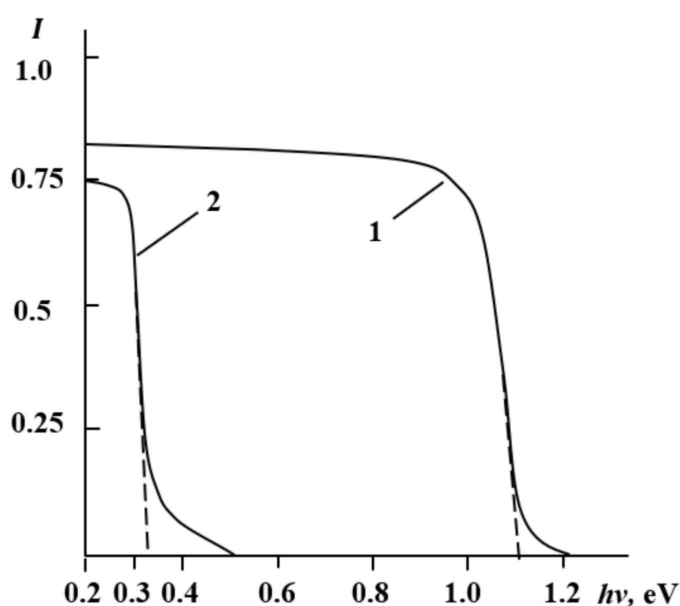

Figure 11. Light absorption spectra: 1 – pure Si (111), 2 – $CrSi_2$/Si (111)

The results of spectroscopic studies illustrating the absorption spectra for Si(111) and Si(111) with a $CrSi_2$ film 62 nm thick are presented in Figure 11. It can be seen that in the case of pure silicon $h\nu \approx 0.22 \div 0.93$ eV, the transmission coefficient $T \approx 0.84$, and the reflection coefficient $R \sim 0.2$. In the case of the $CrSi_2$/Si(111) film in the range $h\nu \approx 0.23$ eV, $T \approx 0.64$ and $R \approx 0.32$. In the second part of the I(hv) dependence, I drops sharply to zero. From the edge of the absorption spectrum, by extrapolating part of the curve onto the $h\nu$ axis, the approximate value of the band gap is determined. It can be seen that $E_g \sim 1.14$ eV for Si(111) and $E_g \sim 0.34$ eV for $CrSi_2$ at room temperature.

4. Conclusion

In this work, thin films of $CrSi_2$ with a purity of 99.5% are formed from a $CrSi_2$ target by a solid-phase ion-plasma method. The morphology and elemental composition of the thin films

were analyzed by scanning electron microscopy using energy dispersive X-ray spectroscopy. Band gap widths of amorphous and polycrystalline $CrSi_2$ thin films were measured using different methods. A comparative analysis was conducted. The optical absorption spectra of the films were studied and as a result approximate band gap values of E_g ~ 1.14 eV for Si(111) and E_g ~ 0.34 eV for $CrSi_2$ were determined at room temperature.

We believe that this research will serve to strengthen scientific research on determining the bandgap of silicide thin films.

Authors'Declaration

The authors declare no conflict of interests regarding the publication of this article.

Author contribution

Author 1, https://orcid.org/0000-0003-1476-6552 (K.T. Dovranov): Formal analysis, Writing - Original Draft, Writing - Review & Editing, Conceptualization, Resources, Investigation

Author 2, https://orcid.org/0000-0003-3275-300X (G.T. Imanova): Formal analysis, Writing - Original Draft, Writing - Review & Editing, Conceptualization, Resources, Investigation, Visualization, Project administration

Author 3, https://orcid.org/0000-0003-3103-7060 (V.V. Loboda): Formal analysis, Writing - Original Draft, Conceptualization, Resources, Investigation, Project administration

Author 4, https://orcid.org/0000 0003 1771 0853 (M.T. Normuradov): Formal analysis, Investigation, Methodology, Data Curation (partially), Conceptualization, Writing - Original Draft, Writing - Review & Editing

Author 5, https://orcid.org/0000-0001-6311-6631 (I.R. Bekpulatov): Investigation, Resources, Writing - Review & Editing, Visualization

References

1. M.T. Normuradov, I.R. Bekpulatov, G.T. Imanova, B.D. Igamov, Advanced Physical Research **4**(3) (2022) 142.
2. I.R. Bekpulatov, G.T. Imanova, T.S. Kamilov, B.D. Igamov, I.K. Turapov, International Journal of Modern Physics B **37**(17) (2023) 22350164.
3. L.N. Agayeva, N.A. Akhmedov, G.T. Imanova, Materials Research Innovations **28**(7) (2024) 550.
4. J. Georgin, D.S.P. Franco, C.G. Ramos, H.N. Tran, A. Benettayeb, G. Imanova, I. Ali, Journal of Molecular Liquids **402** (2024) 124786.
5. I. Ali, G. Imanova, T. Agayev, A. Aliyev, T.A. Kurniawan, M.A. Habila, Radiation Physics and Chemistry **223** (2024) 111902.
6. I. Ali, T. Kon'kova, E. Liberman, A. Gaydukova, T.A. Kurniawan, S.A. Aldossari, G. Imanova, X.Y. Mbianda, Inorganic Chemistry Communications **167** (2024) 112747.
7. I. Ali, G. Imanova, T. Agayev, A. Aliyev, T.A. Kurniawan, M.A. Habila, Radiation Physics and Chemistry **224** (2024) 112002.
8. M. Xiang, N. Wang, L. Sun, L. He, L. Zhong, G. Imanova, S. Komarneni, W. Hu, Separation and Purification Technology **354**(1) (2025) 128667.
9. L. Zhu, S. Zhou, H. Cheng, J. Ma, G. Imanova, S. Komarneni, Journal of Environmental Chemical Engineering **12**(5) (2024) 113591.
10. I. Ali, H. Mahmudov, G. Imanova, T.A. Kurniawan, M.A. Habila, Materials Research Innovations **28**(4) (2024) 1.
11. G. Imanova, Modern Physics Letters B **38**(22) (2024) 2450206.
12. G.T. Imanova, T.N. Agayev, S.H. Jabarov, Modern Physics Letters B **35**(02) (2021) 2150050.
13. B.E. Umirzakov, G.T. Imanova, I.R. Bekpulatov, and I.Kh. Turapov, Modern Physics Letters B **37**(24) (2023) 2350078.

14. B.D. Igamov, G.T. Imanova, A.I. Kamardin, I.R. Bekpulatov, Integrated Ferroelectrics **240**(1) (2024) 53.
15. A.E. Shumskaya, S.N. Lemesonok, O.A. Alisienok, V.E. Kovalev, S.I.Korzan, E.A. Kulesh, G.T. Imanova & S.H. Jabarov, Materials Research Innovations **28**(5) (2024) 379.
16. F.K. Khallokov, G.T. Imanova, S.Kh. Umarov, M.Yu. Tashmetov, N.Z. Gasanov,Z.U. Esanov, I.R. Bekpulatov, Materials Research Innovations (2024) 1.
17. S.H. Jabarov, A.K. Nabiyeva, E.M. Huseynov, Journal Porous Materials **31** (2024) 1811.
18. B.E. Umirzakov, Zh.M. Jumayev, I.R. Bekpulatov, I.Kh. Turapov, G.T. Imanova & N.P. Farmonov, Materials Research Innovations **28**(3) (2024) 1.
19. M.N. Mirzayev, G.T. Imanova, D. Neov, M. Rasoul, I.R. Bekpulatov, F.K. Khallokov, E.P. Popov, K. Hasanov, S. Isayeva, B. Mauyey, D.M. Mirzayeva, F. Tatardar, M. Dinu, G. Kaminski, A. Vladescu, Journal of Porous Materials **31** (2024) 1531.
20. I.R. Bekpulatov, G.T. Imanova, B.E. Umirzakov, K.T. Dovranov, V.V. Loboda, S.H. Jabarov, I.X. Turapov, N.E. Norbutaev, Materials Research Innovations **28**(4) (2024) 221.
21. G. Imanova, S. Jabarov, T. Agayev, Journal Porous Materials **31** (2024) 1135.
22. G.T. Imanova, Advanced Physical Research **2**(2) (2020) 94.
23. B.E. Umirzakov, I.R. Bekpulatov, G.T. Imanova, I.Kh. Turapov, J.M. Jumaev, Eurasian Journal of Physics and Functional Materials **7**(4) (2023) 249.
24. B.D. Igamova, G.T. Imanova, A.I. Kamardin and I.R. Bekpulatov, Integrated ferroelectrics **240**(1) (2024) 53.
25. F.K. Khallokov, G.T. Imanova, S.Kh. Umarov, M.Yu. Tashmetov, N.Z. Gasanov, Z.U. Esanov, I.R. Bekpulatov, Materials Research Innovations (2024) 1.
26. B.D. Igamov, I.R. Bekpulatov, G.T. Imanova, A.I. Kamardin, D.A. Normurodov, Physics and chemistry of solid state **25**(2) (2024) 421.
27. M. Oydinov, B. Igamov, I. Bekpulatov, E. Abdurahmonov, G. Imanova, Chemical Bulletin of Kazakh National University **111**(1-2) (2024) 28.
28. A. Maharramov, N.Q. Shikhaliyev, A. Abdullayeva, G.T. Atakishiyeva, A. Niyazova, V.N. Khrustalev, S.I. Gahramanova, Z. Atioğlu, M. Akkurt, A. Bhattarai, Acta Crystallographica Section E **79**(10) (2023) 905.
29. M. Akkurt, A.M. Maharramov, N.Q. Shikhaliyev, A. Qajar, G.T. Atakishiyeva, I.M. Shikhaliyeva, A.A. Niyazova, A. Bhattari, UNEC Journal of Engineering and Applied Science **3**(1) (2023) 33.
30. Z. Atioglu, M. Akkurt, N.Q. Shikhaliyev, U.F. Askerova, A.A. Niyazova, S. Mlowe, Acta Crystallographica Section E **77**(8) (2021) 829.
31. R.K. Askerov, A.M. Maharramov, A.N. Khalilov, M. Akkurt, A.A. Akobirshoeva, V.K. Osmanov, A.V. Borisov, Acta Crystallographica Section E **76**(7) (2020) 1007.
32. F.N. Naghiyev, V.N. Khrustalev, E.V. Dobrokhotova, M. Akkurt, A.N. Khalilov, A. Bhattarai, I.G. Mamedov, Acta Crystallographica Section E **78**(6) (2022) 568.
33. F.N. Naghiyev, A.V. Pavlova, V.N. Khrustalev, M. Akkurt, A.N. Khalilov, A.A. Akobirshoeva, I.G. Mamedov, Acta Crystallographica Section E **77**(9) (2021) 930.
34. I.R. Bekpulatov, G.T. Imanova, S.H. Jabarov, B.E. Umirzakov, K.T. Dovranov, V.V. Loboda, I.X. Turapov, N.E. Norbutaev, M.I. Sayyed, D.I. Tishkevich and A.V. Trukhanov, Journal of Materials Science: Materials in Electronics **35** (2024).
35. Z.A. Isakhanov, B.E. Umirzakov, G.T. Imanova, Optical Materials: X **24** (2024) 100354.
36. B.D. Igamov, G.T. Imanova, V.V. Loboda, V.V. Zhurikhina, I.R. Bekpulatov, A.I. Kamardin, Optical Materials: X **24** (2024) 100353.
37. R.F. Babayeva, T.G. Naghiyev, Modern Physics Letters B **37**(21) (2023) 2350058.
38. R.S. Madatov, A.S. Alekperov, N.N. Gadzhieva, F.G. Asadov, Sh.A. Allahverdiev, E.G. Asadov, T.G. Naghiyev, Internation J. of Modern Physics B **33**(09) (2019) 1950066.
39. A.P. Abdullayev, R.M. Rzayev, T.G. Naghiyev, J.P. Mammadova, S.S. Aliyev, I.V. Musazade, International Journal of Modern Physics B **37**(28) (2023) 2350248.